Prev. Nutr. Food Sci. 2023;28(4):436-443
https://doi.org/10.3746/pnf.2023.28.4.436
ISSN 2287-8602

Harmine Hydrochloride Induces G2/M Cell Cycle Arrest and Apoptosis in SK-Hep1 Hepatocellular Carcinoma Cells by Regulating Mitogen-Activated Protein Kinases and the PI3K/AKT Pathway

Gi Dae Kim

Department of Food and Nutrition, Kyungnam University, Gyeongnam 51767, Korea

ABSTRACT: Liver cancer is a globally common form of cancer. Thus, novel drugs derived from natural products are needed to reduce the side effects of chemotherapy. The present study aimed to analyze the anticancer properties and effects of harmine hydrochloride (HMH), a water-soluble metabolite of harmine that can be easily absorbed into tissues, in treating liver cancer cells. HMH dose-dependently inhibited cell growth, migration, invasion, and colony formation in SK-Hep1 cells. It also induced G2/M arrest by reducing the expression of p-cdc2, cyclin B1, and Rb (G2/M phase regulatory proteins) in a dose-dependent manner. HMH treatment reduced the expression of caspase-9, caspase-3, PARP, and Bcl-2 and increased the expression of Bax (a proapoptotic protein). Moreover, it increased the production of reactive oxygen species and decreased the intracellular uptake of rhodamine 123 due to mitochondrial dysfunction because of oxidative stress. HMH treatment also upregulated the phosphorylation of JNK, p38, and FOXO3a in SK-Hep1 cells and downregulated the PI3K/AKT signaling pathway. Our findings suggest that HMH may activate the compounds responsible for anticancer effects in hepatocellular carcinoma cells.

Keywords: harmine hydrochloride, hepatocellular carcinoma cells, PI3K/AKT

INTRODUCTION

Liver cancer has high incidence and mortality rates; it is characterized by rapid progression and commonly diagnosed late after onset (Calderaro et al., 2019). Currently, the main treatment methods for liver cancer include surgery and chemotherapy. However, conventional chemotherapy is insufficient and has various side effects (Chau et al., 2006; Lo et al., 2007). Therefore, new and effective chemotherapy drugs, especially those derived from natural products, are urgently needed. Alkaloids, which are commonly found in plants, constitute a class of alkaline organic compounds that contain nitrogen. Most alkaloids have a complex ring structure, with nitrogen possessing significant biological activity. Owing to their high physiological and pharmacological activity, alkaloids are essential and effective ingredients in traditional Chinese herbal medicine (Man et al., 2012). Many alkaloids have been widely used for treating cough, hypertension, inflammation, and various tumors and improving liver function. Harmine, a beta-carboline alkaloid isolated from the seeds of *Peganum harmala*, has been traditionally used as a functional food and medicine (Li et al., 2015). Previous studies have reported that harmine exhibits antiAlzheimer, anticancer, and antiinflammatory properties (Chen et al., 2005; Zhang et al., 2014; Filali et al., 2015; Chen et al., 2022).

Harmine hydrochloride (HMH), a derivative of harmine, improves water solubility and bioavailability when added to beta-carboline alkaloids (Patel et al., 2012). Notably, HMH inhibits gastric and colorectal cancer cell proliferation by regulating cell invasion and migration and inducing apoptosis (Tan et al., 2020; Kim, 2021a). However, studies on the effects of HMH in regulating the invasion, migration, and activation mechanisms of hepatocellular carcinoma (HCC) cells remain insufficient.

Thus, the present study analyzed the anticancer effects and mechanisms of HMH, including the regulation of the invasion and movement of HCC cells.

Received 23 October 2023; Revised 8 November 2023; Accepted 10 November 2023; Published online 31 December 2023
Correspondence to Gi Dae Kim, E-mail: gidaekim@kyungnam.ac.kr

MATERIALS AND METHODS

Cell culture and viability assay

SK-Hep1, a human HCC cell line, was purchased from the American Type Culture Collection. The cells were cultured in Dulbecco's modified Eagle's medium (DMEM) with 10% fetal bovine serum (FBS) and 1% antibiotic-antimycotics at 37°C in a 5% CO_2 incubator. HMH (Sigma-Aldrich; Fig. 1A) was dissolved in 100% dimethyl sulfoxide. Following HMH treatment, the cell viability was assessed using 3-(4,5-dimethylthiazol-2-yl)-2,5-diphenyltetrazolium bromide (MTT) assay, as previously reported (Chae and Kim, 2021). Briefly, the standard medium was removed after cells were placed on 96-well plates and cultured overnight. Thereafter, the medium containing 0~1,000 μM of HMH was added to DMEM and cultured for 24~72 h. Cell viability was determined by measuring the optical density values at 570 nm using a Synergy HTX plate reader (Bio-Tek Instruments, Inc.).

Wound healing assay

Wound healing assay was performed as previously reported (Kim, 2021b). Briefly, the cells in each well were wounded using a pipette tip. Consequently, dead cells were removed by washing with fresh medium. Thereafter, 0, 12.5, 25, and 50 μM of HMH was added to fresh DMEM containing 1% FBS, and the cells were cultured for 24 h. The wound healing area was measured using ImageJ software (National Institutes of Health).

Invasion assay

Invasion assay was performed as previously reported (Ock and Kim, 2021). Briefly, cells were added to 1.5 mL of serum-free DMEM treated with different concentrations of HMH in the upper chamber (Corning), whereas DMEM containing 10% FBS was added to the lower chamber. After culturing for 24 h, cells that invaded the lower chamber were fixed for 30 min in 4% paraformaldehyde. Subsequently, after staining with 0.5% crystal violet solution for 30 min, invasive cells were observed under a microscope and quantified using ImageJ software.

Colony formation assay

Colony formation assay was performed as previously reported (Kim, 2021b). Briefly, cells were seeded in six-well plates by adding 1,000 cells/well to 2 mL of DMEM containing 10% FBS. After culturing for 24 h in medium treated with different concentrations of HMH, the cells were incubated in fresh medium for 14 days, during which the medium was replaced once every 3~4 days. Colony formation was observed and quantified using ImageJ software.

Flow cytometry analysis of cell cycle distribution

The cells were spread on a 100-mm culture dish and cultured for 24 h until >70% cell density was reached. Cell cycle distribution assay was performed as previously reported (Ock and Kim, 2021). Briefly, the cells were cultured with 0, 12.5, 25, and 50 μM of HMH for 24 h. The harvested cells were fixed overnight in 70% cold ethanol at −20°C. Thereafter, the cells were stained with 50 μg/mL of propidium iodide (PI) for 30 min and analyzed using a FACSVantage SE flow cytometer (BD Biosciences) for cell cycle analysis.

Cell apoptosis assay

Apoptosis following HMH treatment in SK-Hep1 cells for 24 h was determined using the Annexin V-FITC Apoptosis

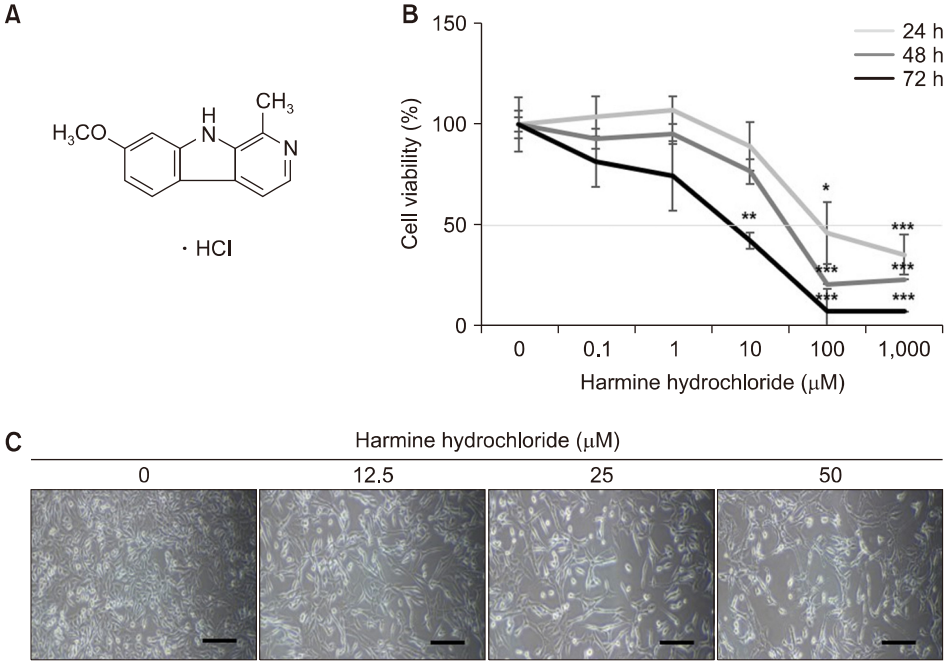

Fig. 1. Effect of harmine hydrochloride (HMH) on the growth of SK-Hep1 cells. (A) Chemical structure of HMH. (B) Cell survival curve according to HMH treatment: after culturing with 0, 1, 10, 100, and 1,000 μM of HMH for 24, 48, and 72 h, cell viability was measured using an MTT assay. (C) Morphological changes: HMH inhibited the growth of SK-Hep1 cells and reduced their density by inhibiting cell growth in a dose-dependent manner. The results are presented as the mean±SD. Student's *t*-test was used to analyze statistical differences between groups (**P*<0.05, ***P*<0.01, ****P*<0.001 with respect to the control group). Cell morphology was visualized using an inverted microscope at 200× magnification. Scale bar, 50 μm.

Detection Kit (BD Pharmingen) in accordance with the manufacturer's instructions (Kim, 2021b). Briefly, the cells were prepared in a binding buffer to 1×10^5 cells/mL concentration and incubated in Annexin V-FITC and PI for 30 min. The stained cells were analyzed using a FACSVantage SE flow cytometer.

Measurement of intracellular reactive oxygen species (ROS) accumulation

ROS production was measured using the fluorescent dye, 2',7'-dichlorodihydrofluorescin diacetate (H_2DCFDA, Molecular Probe). ROS production assay was performed as previously reported (Kim, 2021a). Briefly, the cells were treated with 0, 12.5, 25, and 50 μM of HMH for 24 h. Thereafter, they were stained with 20 μM of H_2DCFDA for 30 min. The amount of intracellular DCF was measured using a FACSVantage SE flow cytometer.

Measurement of mitochondrial membrane potential

The mitochondrial membrane potential was evaluated using rhodamine 123 as previously reported (Kim et al., 2013). After 24 h of HMH treatment, the cells were cultured with 1 μL/mL of rhodamine 123 for 60 min. Then, they were analyzed using a FACSVantage SE flow cytometer with verapamil (20 μM) as a positive control.

Immunoblotting

The cells were treated with HMH (0, 12.5, 25, 50 μM) for 24 h, and the proteins were extracted with a protein extraction solution (Roche Diagnostics GmbH) for 30 min at 4°C (Ock and Kim, 2021). Protein samples were separated using sodium dodecyl-sulfate polyacrylamide gel electrophoresis and transferred onto polyvinylidene fluoride membranes (Bio-Rad Laboratories, Inc.). After blocking membranes with Tris-buffered saline for 1 h, primary antibodies (1:500～1:1,000) were diluted in 5% bovine serum albumin and left to react overnight at 4°C. The membranes were cultured with horseradish peroxidase-conjugated secondary antibodies (1:1,000) for 1 h and detected using the Western Blot Detection Kit (Amersham).

Statistical analyses

The results are presented as mean±standard deviation. Statistical significance ($P<0.05$) was defined using Student's *t*-test. Statistical analyses were performed using IBM SPSS software version 23.0 (IBM Corp.).

RESULTS

HMH inhibits the growth of SK-Hep1 cells

HMH was applied to cells at concentrations ranging from 0 to 1,000 μM for 24～72 h to determine whether HMH has a cell growth inhibitory effect on HCC cells. The IC_{50} values of HMH in SK-Hep1 cells were 98.5, 55.0, and 11.5 μM after HMH treatment for 24, 48, and 72 h, respectively (Fig. 1B). In addition, a statistically significant inhibition of cell proliferation was observed after treatment with 100 μM of HMH for 24, 48, and 72 h ($P<0.05$). After HMH treatment for 72 h, statistically significant results were observed at a concentration of 10 μM ($P<0.01$). In a subsequent analysis based on the IC_{50} values, the changes in cell morphology after 24-h treatment with 50 μM of HMH revealed that 50 μM of HMH exhibited biological activity with low cytotoxicity. Therefore, subsequent experiments were performed using 50 μM of HMH (Fig. 1C).

HMH inhibits migration, invasion, and colony formation in SK-Hep1 cells

The cells were scratched from a culture dish after reaching approximately 70～80% confluence for migration analysis. Notably, the amount of FBS in the cell culture medium was reduced from 10% to 1%, and the cells were treated with 0, 12.5, 25, and 50 μM of HMH for 24 h. The wound healing area was 78.1% in the control group and 43.2% and 39.5% in the 25 and 50 μM HMH treatment groups, respectively, indicating that migration was significantly inhibited ($P<0.05$; Fig. 2A). The cells were treated with 0, 12.5, 25, and 50 μM of HMH for 24 h in a chamber with 8-μm polycarbonate membranes to determine the degree of invasion of HCC cells. Then, the number of cells migrating to the lower chamber was measured and compared with that of the control group (Fig. 2B). Compared with that of the control group, the number of invading cells in the 25 and 50 μM HMH treatment groups was significantly reduced to 23.5% and 13.8%, respectively ($P<0.01$). Next, HMH was applied at 0, 12.5, 25, and 50 μM concentrations for 24 h to evaluate the inhibitory effect of HMH on colony formation. After the HMH-containing medium was removed, the colony formation ability was evaluated by culturing the cells in fresh DMEM for 14 days (Fig. 2C). Compared with that of the control group, the colony formation ability in SK-Hep1 cells was significantly inhibited by 58.2% and 22.8% in the 25 and 50 μM HMH treatment groups, respectively ($P<0.05$).

HMH induces G2/M arrest and apoptosis in SK-Hep1 cells

SK-Hep1 cells were treated with 0～50 μM of HMH for 24 h. Notably, at 25 μM HMH concentration, the number of cells in the G0/G1 phase decreased, whereas that in the G2/M phase increased by 37.76% compared with 15.98% in the control group (Fig. 3A and B). In addition, at 50 μM HMH concentration, the number of cells in the sub-G1 phase increased to 11.9% compared with 1.22% in the control group. Additionally, G2/M phase-related cell cycle

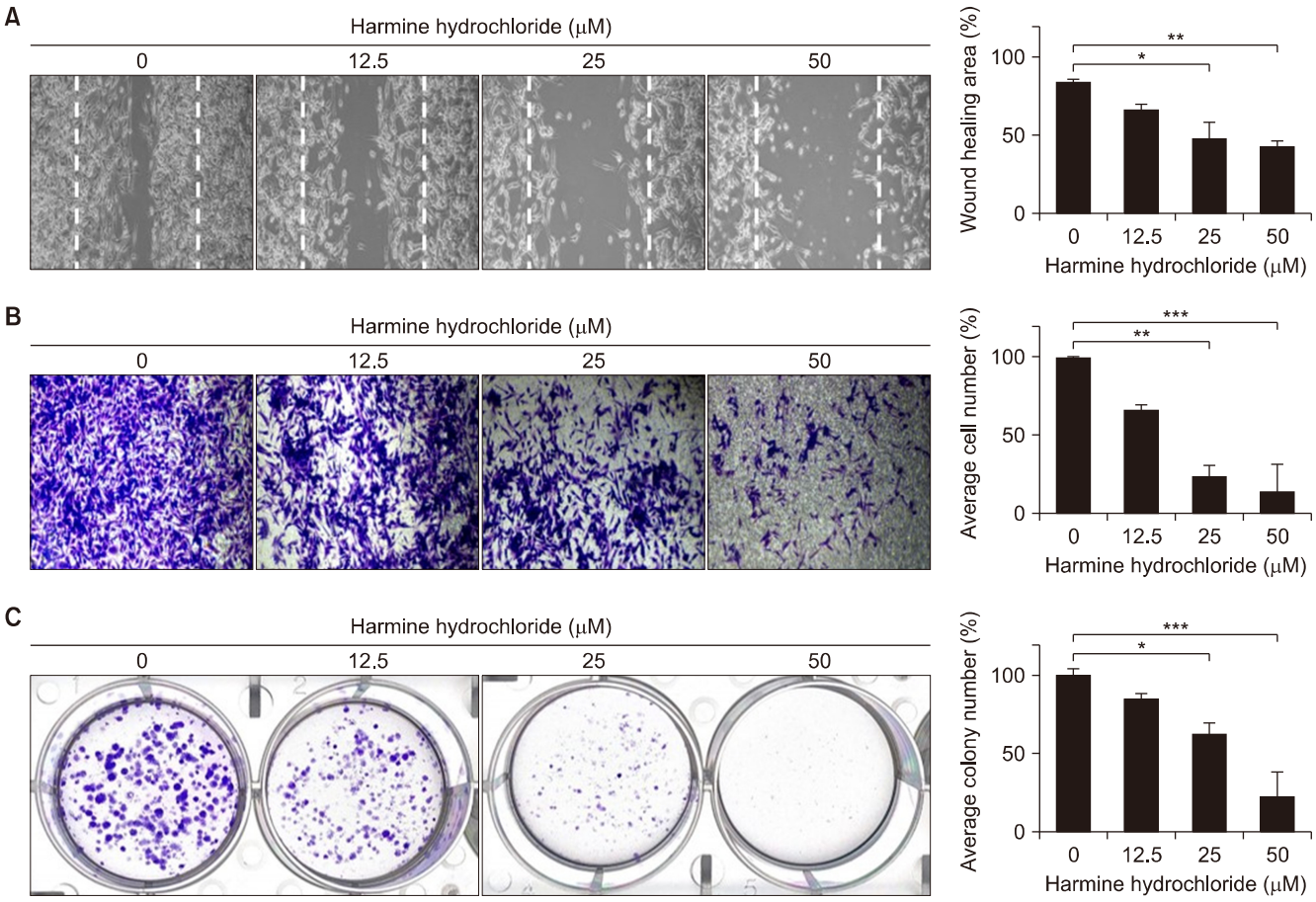

Fig. 2. Effect of harmine hydrochloride (HMH) on migration, invasion, and colony formation. (A) Cells after confluent growth in six-well plates were scratch-wounded and treated with 0~50 μM of HMH to measure the migration area after 24 h. (B) Cells were placed in the upper chamber with 1.5 mL of serum-free Dulbecco's modified Eagle's medium (DMEM), and DMEM containing 10% fetal bovine serum was added to the lower chamber. After culturing for 24 h, non-invading cells in the upper chamber were removed using a cotton swab, and cells invading the lower chamber were fixed using 4% paraformaldehyde and stained with 0.5% crystal violet solution. Subsequently, invasive cells were observed under a microscope. (C) Cells were seeded in six-well plates and treated with 0~50 μM of HMH for 24 h, and then, the medium was removed. Thereafter, cells were cultured for 14 days while replacing the medium with fresh medium every 3~4 days. Cells were fixed with methanol and stained with 0.5% crystal violet to determine colony formation. They were examined under a microscope, and wound areas and number of colonies were determined using ImageJ software. The results are presented as the mean±SD. Student's *t*-test was used to analyze statistical differences between groups (**P*<0.05, ***P*<0.01, ****P*<0.001 with respect to the control group). Cell morphology was visualized using an inverted microscope at 200× magnification.

regulatory proteins were determined using Western blot analysis (Fig. 3C). HMH increased the expression of cell cycle regulators p53 and p21, whereas it dose-dependently decreased the expression of G2/M phase regulatory proteins p-cdc2, cdc2, and cyclin B1. In addition, a decrease in the expression of Rb, a cell proliferation regulatory protein, was observed.

In the cell cycle regulation analysis, treatment with up to 25 μM of HMH induced G2/M arrest, whereas treatment with 50 μM of HMH increased the number of cells in the sub-G1 phase. Therefore, an Annexin V-FITC/PI double staining assay was performed to determine whether HMH treatment induces apoptosis. Notably, the apoptotic cell population significantly increased to 26.92% in the 50 μM HMH treatment group ($P<0.05$; Fig. 4A and B). Antiapoptotic proteins such as caspase-9, caspase-3, PARP, and Bcl-2 and proapoptotic protein (Bax) were identified using Western blot analysis to study the fundamental mechanism underlying apoptosis induction (Fig. 4C). Apoptotic proteins, such as caspase-9, caspase-3, and PARP, were cleaved depending on the HMH concentration. HMH treatment dose-dependently decreased the expression of Bcl-2 and increased the expression of Bax following apoptosis induction. Additionally, ROS production increased to 45.0% in the 50 μM HMH treatment group compared with 3.9% in the control group (Fig. 4D). Next, we investigated whether ROS production by HMH is associated with the regulation of intracellular mitochondrial membrane potential. We detected 90.5% active accumulation of rhodamine 123 in positive control (20 μM verapamil) cells compared with the control group (IgG, negative control). However, rhodamine accumulation was reduced to 71.8% after treatment with 50 μM of HMH (Fig. 4E). The cellular uptake of rhodamine 123 was signifi-

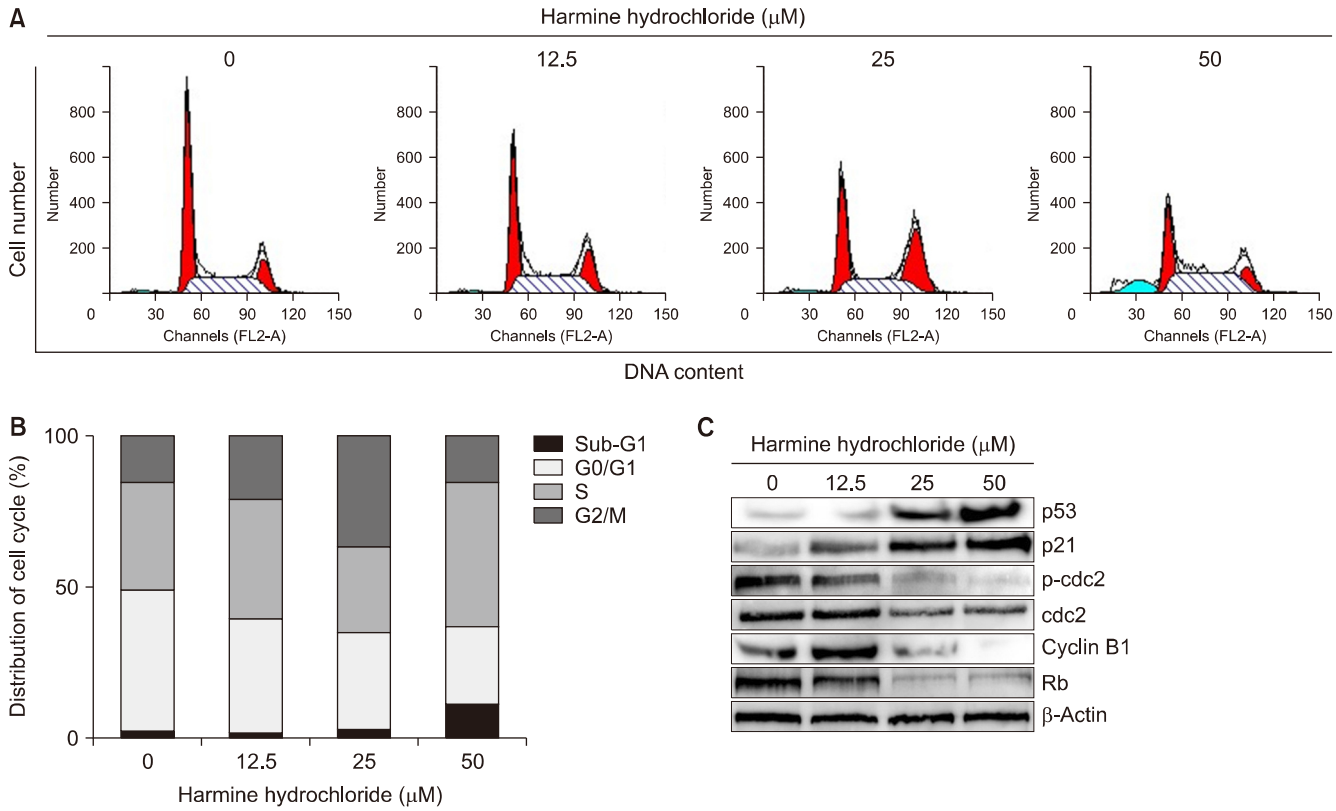

Fig. 3. Effect of harmine hydrochloride (HMH) on cell cycle progression. (A) After treating cells with 0, 12.5, 25, and 50 μM of HMH for 24 h, flow cytometric analyses were performed on cells stained with propidium iodide to determine cell cycle progression. (B) Cumulative cell distribution in the Sub-G1, G0/G1, S, and G2/M phases of the cell cycle after HMH treatment. (C) The expression levels of G2/M-related proteins such as p53, p21, p-cdc2, cdc2, cyclin B1, and Rb were determined using Western blot analysis. β-Actin was used as an internal control.

cantly reduced possibly because of oxidative stress-induced mitochondrial dysfunction, suggesting that HMH affects the mitochondrial membrane potential.

HMH regulates mitogen-activated protein kinases (MAPKs) and the PI3K/AKT signaling pathway

JNK and p38, which are representative MAPKs, are kinases that link extracellular signals necessary for regulating cell growth, differentiation, migration, and apoptosis. HMH increased the phosphorylation of JNK, p38, and FOXO3a in a dose-dependent manner (Fig. 5A). We investigated whether HMH treatment affected the PI3K/AKT signaling pathway in SK-Hep1 cells (Fig. 5B). Western blot analysis was performed to evaluate the inhibitory effect of protein expression following the treatment of SK-Hep1 cells with 0, 12.5, 25, and 50 μM of HMH for 24 h. HMH treatment decreased the phosphorylation of PI3K, AKT, and mTOR. These results show that JNK, p38, and the PI3K/AKT signaling pathway mediate the inhibition of cell proliferation and migration and induction of apoptosis following HMH treatment.

DISCUSSION

Developing anticancer drugs with various physiological activities and low toxicity from natural products is of significant interest. In this study, HMH, a water-soluble and stable metabolite of harmine, was used to treat HCC cells to determine its anticancer properties and study its underlying mechanism of action. HMH treatment reduced the cell viability and inhibited the migration, invasion, and colony formation of SK-Hep1 cells, all of which are characteristics of cancer cells. In addition, HMH treatment resulted in G2/M arrest and apoptosis induction.

Cyclin and cyclin-dependent kinase (CDK) complexes play an important role in regulating cell cycle progression. There are four major checkpoints in cell cycle progression: G1/S, S, G2/M, and spindle assembly checkpoints (Sánchez and Dynlacht, 2005). The G1/S phases are regulated by CDK4, cyclin D1, CDK2, and cyclin E, whereas the G2/M phases are regulated by CDK2, cyclin A, cdc2, and cyclin B. In particular, the cyclin B1/cdc2 complex identified in this study has a crucial function in controlling the G2/M transition. The CDK inhibitor $p21^{Waf1/Cip1}$ inactivates the cyclin B1/cdc2 complex in p53-dependent sustained G2/M arrest (Smith et al., 2020). In this study, HMH induced G2/M cell cycle arrest up to a concentra-

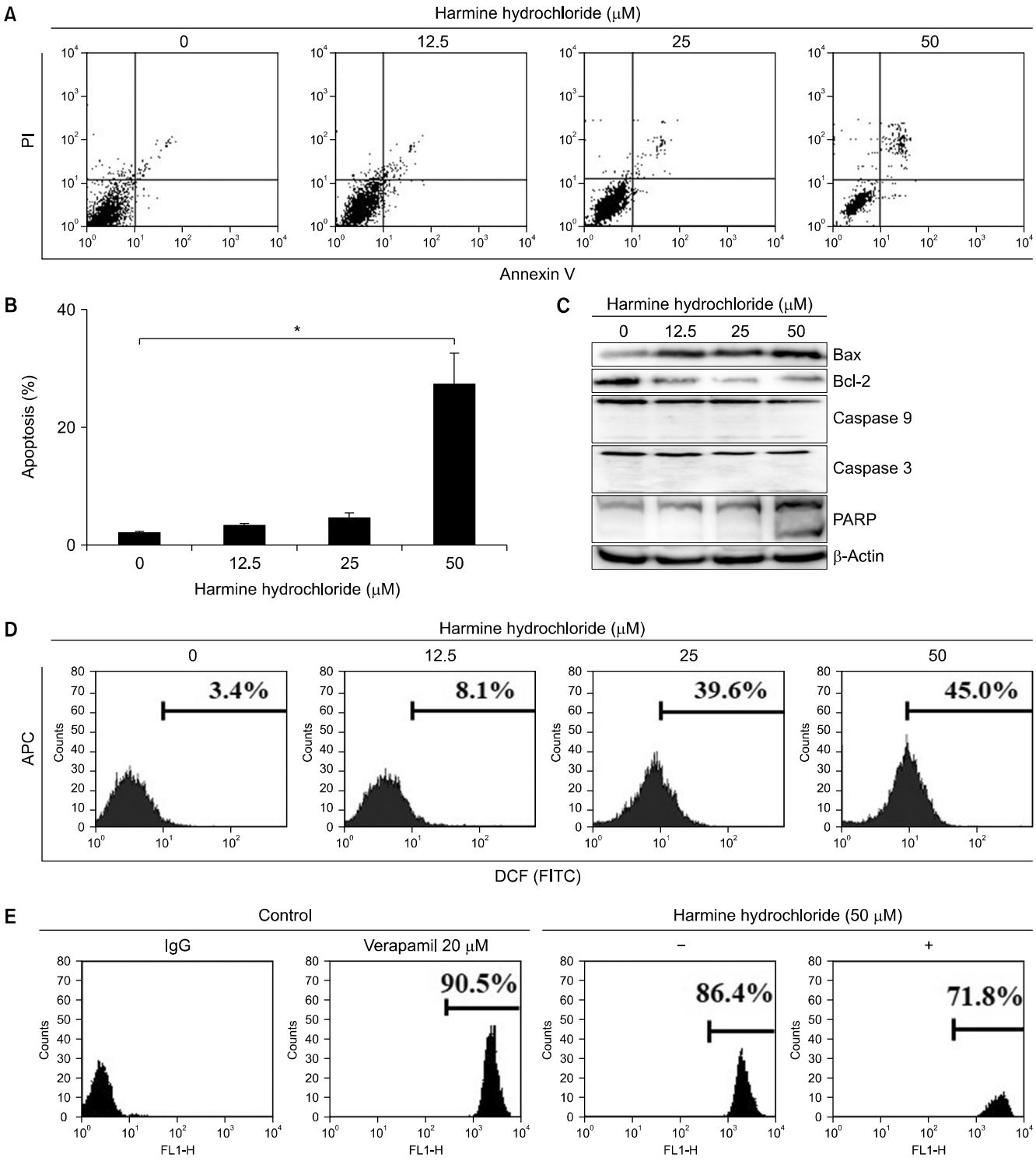

Fig. 4. Effects of harmine hydrochloride (HMH) on reactive oxygen species (ROS) production and mitochondrial membrane potential following apoptosis induction. (A and B) Cells were treated with 0, 12.5, 25, and 50 μM of HMH for 24 h; stained with Annexin V and propidium iodide (PI); and analyzed with a FACSVantage SE flow cytometer (BD Biosciences). (C) The expression of pro-/antiapoptotic proteins in cells where apoptosis was induced by HMH treatment was analyzed using Western blot analysis. (D) ROS generation was quantified by measuring DCF using 2′,7′-dichlorofluorescin diacetate in cells exposed to 0, 12.5, 25, and 50 μM of HMH for 24 h. (E) After treatment with HMH or verapamil (positive control) for 24 h, cells were cultured with rhodamine 123 and analyzed with a flow cytometer. The results are presented as the mean±SD. Student's *t*-test was used to analyze statistical differences between groups (**P*<0.05 with respect to the control group).

tion of 25 μM in SK-Hep1 cells. Furthermore, immunoblotting results indicated that HMH substantially upregulated p53 and p21 at the protein level in SK-Hep1 cells and downregulated cyclin B1, p-cdc2, and Rb.

Apoptosis is induced in several ways, including the receptor pathway, mitochondrial pathway, and endoplasmic

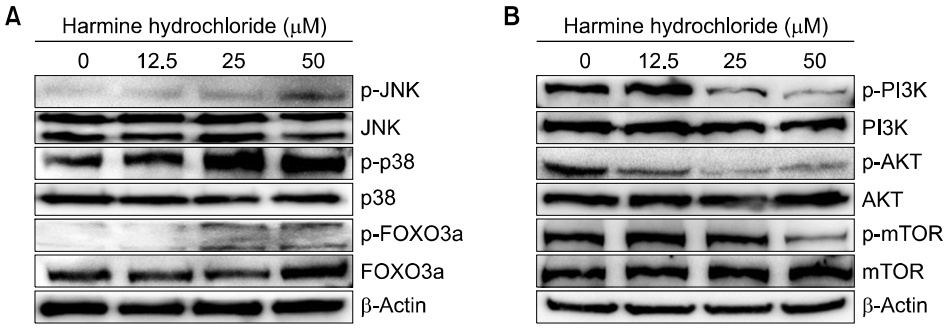

Fig. 5. Action of harmine hydrochloride (HMH) on mitogen-activated protein kinases (MAPKs) and the PI3K/AKT signaling pathway. The expression of MAPKs (A) and PI3K/AKT-related proteins (B) after treatment with 0, 12.5, 25, and 50 μM of HMH for 24 h was determined using Western blot analysis. β-Actin was used as an internal control.

reticulum stress-mediated death, under normal physiological or pathological conditions (Khan et al., 2014). In particular, various factors downregulate survival proteins and upregulate apoptotic proteins in the mitochondrial apoptosis pathway, decreasing the mitochondrial membrane potential and inducing cytochrome c release from mitochondria. Cytochrome c in the cytoplasm triggers caspase-9, caspase-3, and PARP degradation, ultimately leading to apoptosis (Gogvadze et al., 2009). Apoptosis is regulated by reducing the expression of antiapoptotic proteins on the mitochondrial membrane, such as Bcl-2, which play an essential role, whereas the expression of proapoptotic proteins, such as Bax, increases or remains unchanged, which induces apoptosis (Zhou et al., 2011). The results of our flow cytometry analysis confirmed that the ratio of apoptotic SK-Hep1 cells increased with HMH treatment. In addition, the results of Western blot analysis showed that HMH treatment increased the expression of Bax and decreased the expression of caspase-9, caspase-3, PARP, and Bcl-2, thereby inducing apoptosis. In addition, ROS play an essential role in the mitochondrial cell death pathway. Endogenous oxidative stress is high in cancer cells. Notably, under pathological conditions, excessive ROS can damage DNA and inhibit cancer growth, leading to cell cycle arrest and apoptosis (Simon et al., 2000; Chen et al., 2017). In the present study, an increase in ROS production was observed following HMH treatment.

JNK and p38 MAPK play vital roles in regulating inflammation, cell growth and differentiation, cell cycle, cell proliferation, apoptosis, and autophagy (Brancho et al., 2005; Dhanasekaran and Reddy, 2008). Activated JNKs are translocated into mitochondria, decreasing the phosphorylation of Bcl-2 (an antiapoptotic protein) and increasing that of Bax, leading to cell death (Jeong et al., 2008). PI3K/AKT is a crucial intracellular signaling pathway. It plays a vital role in proliferation, growth and metabolism, and cell survival, which are closely related to tumor development and progression in humans, by affecting the activity of downstream molecules (Zhang et al., 2015). FOXO3a is an important target of the PI3K/AKT signaling pathway (Sunters et al., 2003), which promotes the expression of target genes such as p21, p27, p53, and cyclins D and B and regulates the cell cycle, which in turn inhibits cancer cell growth (Taniguchi et al., 2019; Nasimian et al., 2020).

Our results show that HMH treatment increased JNK and p38 expression, inhibited PI3K and AKT phosphorylation, and activated FOXO3a response in SK-Hep1 cells. Notably, the inactivation of the PI3K/AKT pathway and activation of JNK and p38 triggered FOXO3a expression and regulated the expression of p53, p21, and cyclin B1, resulting in G2/M cell cycle arrest. These results reveal the anticancer bioactivity of HMH in HCC cells.

FUNDING

This work was supported by the National Research Foundation of Korea (NRF) grant funded by the Korean government (MSIT) (No. NRF-2020R1F1A1072191).

AUTHOR DISCLOSURE STATEMENT

The author declares no conflict of interest.

REFERENCES

Brancho D, Ventura JJ, Jaeschke A, Doran B, Flavell RA, Davis RJ. Role of MLK3 in the regulation of mitogen-activated protein kinase signaling cascades. Mol Cell Biol. 2005. 25:3670-3681.

Calderaro J, Ziol M, Paradis V, Zucman-Rossi J. Molecular and histological correlations in liver cancer. J Hepatol. 2019. 71:616-630.

Chae WO, Kim GD. Dioscin decreases breast cancer stem-like cell proliferation via cell cycle arrest by modulating p38 mitogen-activated protein kinase and AKT/mTOR signaling pathways. J Cancer Prev. 2021. 26:183-194.

Chau GY, Lui WY, Tsay SH, Chao Y, King KL, Wu CW. Postresectional adjuvant intraportal chemotherapy in patients with hepatocellular carcinoma: a case-control study. Ann Surg Oncol. 2006. 13:1329-1337.

Chen Q, Chao R, Chen H, Hou X, Yan H, Zhou S, et al. Antitumor and neurotoxic effects of novel harmine derivatives and structure-activity relationship analysis. Int J Cancer. 2005. 114:675-682.

Chen X, Dai X, Zou P, Chen W, Rajamanickam V, Feng C, et al. Curcuminoid EF24 enhances the anti-tumour activity of Akt inhibitor MK-2206 through ROS-mediated endoplasmic reticu-

lum stress and mitochondrial dysfunction in gastric cancer. Br J Pharmacol. 2017. 174:1131-1146.
Chen ZY, Li J, Zhu SD, Li ZD, Yu JL, Wu J, et al. Harmine reinforces the effects of regorafenib on suppressing cell proliferation and inducing apoptosis in liver cancer cells. Exp Ther Med. 2022. 23:209. https://doi.org/10.3892/etm.2022.11132
Dhanasekaran DN, Reddy EP. JNK signaling in apoptosis. Oncogene. 2008. 27:6245-6251.
Filali I, Bouajila J, Znati M, Bousejra-El Garah F, Ben Jannet H. Synthesis of new isoxazoline derivatives from harmine and evaluation of their anti-Alzheimer, anti-cancer and anti-inflammatory activities. J Enzyme Inhib Med Chem. 2015. 30:371-376.
Gogvadze V, Orrenius S, Zhivotovsky B. Mitochondria as targets for cancer chemotherapy. Semin Cancer Biol. 2009. 19:57-66.
Jeong HS, Choi HY, Choi TW, Kim BW, Kim JH, Lee ER, et al. Differential regulation of the antiapoptotic action of B-cell lymphoma 2 (Bcl-2) and B-cell lymphoma extra long (Bcl-xL) by c-Jun N-terminal protein kinase (JNK) 1-involved pathway in neuroglioma cells. Biol Pharm Bull. 2008. 31:1686-1690.
Khan KH, Blanco-Codesido M, Molife LR. Cancer therapeutics: Targeting the apoptotic pathway. Crit Rev Oncol Hematol. 2014. 90:200-219.
Kim GD, Oh J, Park HJ, Bae K, Lee SK. Magnolol inhibits angiogenesis by regulating ROS-mediated apoptosis and the PI3K/AKT/mTOR signaling pathway in mES/EB-derived endothelial-like cells. Int J Oncol. 2013. 43:600-610.
Kim GD. Harmine hydrochloride triggers G2/M Cell cycle arrest and apoptosis in HCT116 cells through ERK and PI3K/AKT/mTOR signaling pathways. Prev Nutr Food Sci. 2021a. 26:445-452.
Kim GD. Ursolic acid decreases the proliferation of MCF-7 cell-derived breast cancer stem-like cells by modulating the ERK and PI3K/AKT signaling pathways. Prev Nutr Food Sci. 2021b. 26:434-444.
Li S, Wang A, Gu F, Wang Z, Tian C, Qian Z, et al. Novel harmine derivatives for tumor targeted therapy. Oncotarget. 2015. 6:8988-9001.
Lo CM, Liu CL, Chan SC, Lam CM, Poon RT, Ng IO, et al. A randomized, controlled trial of postoperative adjuvant interferon therapy after resection of hepatocellular carcinoma. Ann Surg. 2007. 245:831-842.
Man S, Gao W, Wei C, Liu C. Anticancer drugs from traditional toxic Chinese medicines. Phytother Res. 2012. 26:1449-1465.
Nasimian A, Farzaneh P, Tamanoi F, Bathaie SZ. Cytosolic and mitochondrial ROS production resulted in apoptosis induction in breast cancer cells treated with Crocin: The role of FOXO3a, PTEN and AKT signaling. Biochem Pharmacol. 2020. 177:113999. https://doi.org/10.1016/j.bcp.2020.113999
Ock CW, Kim GD. Harmine hydrochloride mediates the induction of G2/M cell cycle arrest in breast cancer cells by regulating the MAPKs and AKT/FOXO3a signaling pathways. Molecules. 2021. 26:6714. https://doi.org/10.3390/molecules26216714
Patel K, Gadewar M, Tripathi R, Prasad SK, Patel DK. A review on medicinal importance, pharmacological activity and bioanalytical aspects of beta-carboline alkaloid "Harmine". Asian Pac J Trop Biomed. 2012. 2:660-664.
Sánchez I, Dynlacht BD. New insights into cyclins, CDKs, and cell cycle control. Semin Cell Dev Biol. 2005. 16:311-321.
Simon HU, Haj-Yehia A, Levi-Schaffer F. Role of reactive oxygen species (ROS) in apoptosis induction. Apoptosis. 2000. 5:415-418.
Smith HL, Southgate H, Tweddle DA, Curtin NJ. DNA damage checkpoint kinases in cancer. Expert Rev Mol Med. 2020. 22:e2. https://doi.org/10.1017/erm.2020.3
Sunters A, Fernández de Mattos S, Stahl M, Brosens JJ, Zoumpoulidou G, Saunders CA, et al. FoxO3a transcriptional regulation of Bim controls apoptosis in paclitaxel-treated breast cancer cell lines. J Biol Chem. 2003. 278:49795-49805.
Tan B, Li Y, Zhao Q, Fan L, Zhang M. The impact of Harmine hydrochloride on growth, apoptosis and migration, invasion of gastric cancer cells. Pathol Res Pract. 2020. 216:152995. https://doi.org/10.1016/j.prp.2020.152995
Taniguchi K, Ii H, Kageyama S, Takagi H, Chano T, Kawauchi A, et al. Depletion of gamma-glutamylcyclotransferase inhibits cancer cell growth by activating the AMPK-FOXO3a-p21 axis. Biochem Biophys Res Commun. 2019. 517:238-243.
Zhang H, Sun K, Ding J, Xu H, Zhu L, Zhang K, et al. Harmine induces apoptosis and inhibits tumor cell proliferation, migration and invasion through down-regulation of cyclooxygenase-2 expression in gastric cancer. Phytomedicine. 2014. 21:348-355.
Zhang J, Yu XH, Yan YG, Wang C, Wang WJ. PI3K/Akt signaling in osteosarcoma. Clin Chim Acta. 2015. 444:182-192.
Zhou F, Yang Y, Xing D. Bcl-2 and Bcl-xL play important roles in the crosstalk between autophagy and apoptosis. FEBS J. 2011. 278:403-413.